Diagnostic Accuracy Study

Medicine®

OPEN

The Usefulness of Maximum Standardized Uptake Value at the Delayed Phase of Tc-99m sestamibi single-photon emission computed tomography/computed tomography for Identification of Parathyroid Adenoma and Hyperplasia

Hoon Young Suh, MD, MS[a,b], Hee Young Na, MD[c], So Yeon Park, MD, PhD[c], June Young Choi, MD, PhD[d], Young So, MD, PhD[e], Won Woo Lee, MD, PhD[a,f,*], K-SPECT Group

Abstract

Tc-99m sestamibi single-photon emission computed tomography/computed tomography (SPECT/CT) has been used to help surgeons explore the location of parathyroid diseases, but quantitative parameters have not been systemically investigated for this purpose. We aimed to establish objective criteria for adenoma and hyperplasia using the standardized uptake value (SUV) in patients with hyperparathyroidism.

Thirty-nine hyperparathyroid patients (male/female: 17/22, age: 58.33 ± 11.69 years) with at least 1 uptake-positive lesion of any degree by visual assessment in preoperative Tc-99m sestamibi quantitative SPECT/CT were included from Oct 2015 to Oct 2017. Pathologically, 44 lesions (32 adenomas and 12 hyperplasia) were identified. All patients experienced normalized levels of intact parathyroid hormone immediately after surgery. Quantitative SPECT/CT was performed at 10 minute and 2 hour post injection of Tc-99m sestabmibi (dose = 740 MBq), and maximum SUV (SUVmax) was measured for the parathyroid lesions. Experienced pathologists evaluated the percentage cellular proportions of chief cells, oxyphil cells, and clear cells.

SUVmax (g/mL) of adenomas, hyperplasia, and reference thyroid tissue were 12.92 ± 6.68, 7.90 ± 5.49, and 7.01 ± 2.62 at 10 min (early phase), decreasing to 7.46 ± 5.66, 4.65 ± 3.14, and 2.21 ± 1.07 at 2 hour (delayed phase), respectively. The adenomas showed significantly higher SUVmax than both the hyperplasia ($P = .0131$) and reference thyroid tissue ($P < .0001$) along the early and delayed phases, but the SUVmax of the hyperplasia did not differ from that of the reference thyroid tissue ($P = .4196$). The adenomas and hyperplasia were discriminated from the reference thyroid tissue using a cutoff SUVmax of 3.26 at the delayed phase. The adenomas had lower %proportions of oxyphil cells than the hyperplasia ($P = .0054$), but its SUVmax at the delayed phase was positively correlated with the %proportions of mitochondria-abundant oxyphil cells (rho = 0.418, $P = .0173$). The hyperplasia showed no correlation between SUVmax and cellular proportions.

SUVmax at the delayed phase in the Tc-99m sestamibi quantitative SPECT/CT was useful for the identification and differentiation of parathyroid lesions causing hyperparathyroidism.

Editor: Nagabhushan Seshadri.

This work was supported in part by the Basic Science Research Program through the National Research Foundation of Korea funded by the Ministry of Education (2018R1D1A1A09081961) and by the Korean Society of Nuclear Medicine Clinical Trial Network (KSNM CTN) working group funded by the Korean Society of Nuclear Medicine (KSNM-CTN-2017-01-01).

The authors have no conflicts of interest to disclose.

The datasets generated during and/or analyzed during the current study are available from the corresponding author on reasonable request.

[a] Department of Nuclear Medicine, Seoul National University Bundang Hospital, Seoul National University College of Medicine, [b] Department of Molecular Medicine and Biopharmaceutical Sciences, Graduate School of Convergence Science and Technology, Seoul National University, [c] Department of Pathology, [d] Department of Surgery, Seoul National University Bundang Hospital, Seoul National University College of Medicine, [e] Department of Nuclear Medicine, Konkuk University Medical Center, Konkuk University School of Medicine, [f] Institute of Radiation Medicine, Medical Research Center, Seoul National University, Seoul, Korea.

[*] Correspondence: Won Woo Lee, Department of Nuclear Medicine, Seoul National University Bundang Hospital, Seoul National University College of Medicine 82, Gumi-ro 173 Beon-gil, Bundang-gu, Seongnam-si, Gyeonggi-do 13620, Korea (e-mail: wwlee@snu.ac.kr).

How to cite this article: Suh HY, Na HY, Park SY, Choi JY, So Y, Lee WW, K-SPECT Group. The Usefulness of Maximum Standardized Uptake Value at the Delayed Phase of Tc-99m sestamibi single-photon emission computed tomography/computed tomography for identification of parathyroid adenoma and hyperplasia. Medicine 2020;99:28(e21176).

Received: 25 March 2020 / Received in final form: 21 May 2020 / Accepted: 7 June 2020

http://dx.doi.org/10.1097/MD.0000000000021176

Abbreviations: ANOVA = analysis of variance, PTH = parathyroid hormone, ROI = region-of-interest, SPECT/CT = single-photon emission computed tomography/computed tomography, SUV = standardized uptake value, VOI = volume-of-interest.

Keywords: single-photon emission computed tomography, computed tomography, parathyroid adenoma, parathyroid hyperplasia, standardized uptake value

Key Points

- Question: Is there an objective SUV criterion for parathyroid adenoma and hyperplasia in quantitative SPECT/CT using Tc-99m sestamibi?
- Pertinent findings: In this retrospective study, the SUVmax of 3.26 at the delayed phase SPECT/CT was accurate enough to identify/differentiate parathyroid lesions that cause hyperparathyroidism. In addition, SUVmax of 7.13 was efficient in differentiation between parathyroid adenoma and hyperplasia.
- Implications for patient care: Accurate preoperative localization of parathyroid lesions may be possible using the quantitative parameter of SPECT/CT.

1. Introduction

Hyperparathyroidism manifests as an uncontrolled elevation of parathyroid hormone (PTH) and hypercalcemia. Primary hyperparathyroidism arises from parathyroid adenomas, hyperplasia (as a key component of multiple endocrine neoplasia syndrome), and carcinomas. Single parathyroid adenomas are the most common (80%–95%) cause of primary hyperparathyroidism.[1–4] Secondary hyperparathyroidism is initially triggered by the hypocalcemia of chronic kidney disease and manifests as parathyroid hyperplasia. At a later stage, the hyperplastic parathyroid achieves autonomy, resulting in tertiary hyperparathyroidism, which features hypercalcemia.[5,6] Primary hyperparathyroidism and medically-intractable tertiary hyperparathyroidism are the best candidates for surgical resection.[7,8]

Accurate preoperative localization of parathyroid lesions remains an unmet need of surgeons. Conventional imaging modalities like computed tomography (CT) and magnetic resonance imaging have had limited success in preoperative localization. For nuclear imaging studies, dual-isotope (e.g., Tl-201 and Tc-99m pertechnetate) subtraction studies or dual-phase Tc-99m sestamibi scintigraphy are recommended by the Society of Nuclear Medicine.[9] As the practice of dual-isotope subtraction is complex, dual-phase Tc-99m sestamibi scintigraphy is considered appropriate for nuclear imaging of hyperparathyroidism.[10,11] Recently, single-photon emission CT/CT (SPECT/CT) using Tc-99m sestamibi has demonstrated usefulness for localizing parathyroid lesions.[12–14] Functional imaging (SPECT) and anatomical imaging (CT) work together for parathyroid lesion detection. However, the optimal protocol for Tc-99m sestamibi SPECT/CT has yet to be determined.[15–17] Some researchers favor early imaging (5–15 min),[15] while others advocate delayed imaging (1.5–3 h).[14,18]

With recent technological developments in radioactivity correction, SPECT/CT is no longer a mere nuclear imaging method but a truly quantitative imaging tool capable of generating voxels in the kBq/mL.[19,20] Standardized uptake value (SUV) is being actively investigated in a variety of SPECT/CT studies.[21–30] Particularly for Tc-99m-based radiopharmaceuticals, the SPECT/CT is now comparable to positron emission tomography for quantitation of radioactivity.[31] However, no quantitative Tc-99m sestamibi SPECT/CT study has systemically investigated the identification of parathyroid lesions. Quantitative assessment of parathyroid lesions may enable determination of the optimal SPECT/CT protocol, which currently has no consensus.[9,15]

In this study of quantitative Tc-99m sestamibi SPECT/CT, we evaluated the SUV of the pathologically proven parathyroid adenomas and hyperplasia, using thyroid tissue as a reference. Additionally, we correlated the SUV with pathologic findings about cellular proportion. We aimed to establish quantitative SUV criteria for adenoma and hyperplasia using Tc-99m sestamibi SPECT/CT in patients with hyperparathyroidism.

2. Materials and Methods

2.1. Patients

Fifty-three consecutive patients with hyperparathyroidism, who underwent preoperative Tc-99m sestamibi quantitative SPECT/CT and surgical exploration in a hospital between Oct 2015 and Oct 2017, were retrospectively included. Hyperparathyroidism was defined as an elevated blood level of PTH and calcium above the reference ranges of 8–76 pg/mL and 8.8–10.5 mg/dL for PTH and calcium, respectively. As the thyroid served as reference tissue here, we excluded 9 patients with thyroid abnormalities: thyroid nodule/cancer (n = 7) and previous unilateral thyroidectomy (n = 2). We also excluded 5 patients and their 8 lesions (4 adenomas, 4 hyperplasia) because the parathyroid lesions were indistinguishable from background tissues by visual assessment in the Tc-99m sestamibi SPECT/CT. Ultimately, 39 patients (men/women: 17/22, age: 58.33 ± 11.69 years) with total 44 lesions (32 adenomas, 12 hyperplasia) were enrolled. Surgery was performed 40.89 ± 61.08 days (range: 1–292 days) after the SPECT/CT, and all patients experienced PTH normalization 7.33 ± 27.12 days after the operation (Table 1). The study has been approved by the institutional review board, and the need for written informed consent was waived.

2.2. Quantitative SPECT/CT of Tc-99m sestamibi

The SPECT/CT was performed using dual-head SPECT/CT scanners (NMCT/670 or NMCT/670Pro, GE Healthcare) equipped with low-energy high-resolution collimators. The protocol consisted of an early scan (planar and SPECT/CT) at 10 minutes and a delayed scan (planar and SPECT/CT) at 2 hours post-injection of 740 MBq (20 mCi) of Tc-99m sestamibi (TechneScan Sestamibi, Mallinckrodt Inc.). The acquisition settings of the early and delayed scans were the same. The planar scan was obtained for 5 minutes with neck extension. The patients then underwent quantitative SPECT/CT. For the SUV

Table 1

Characteristics of the patients (n = 39).

	Patients with adenoma (n = 32)	Patients with hyperplasia (n = 7)
Gender, male:female	14:18	3:4
Age, (yr)	61 ± 11	47 ± 9
Pre-op iPTH (pg/mL)	186 ± 141	242 ± 266
Post-op iPTH (pg/mL)	20 ± 12	26 ± 28
Underlying cause		
Primary (idiopathic)	32	0
Primary (MEN type 1)	0	3
Tertiary (post KTP)	0	4
No. of lesions per patient		
1	32	5
2	0	0
3	0	1
4	0	1

Data are presented as mean ± standard deviation.
iPTH = intact parathyroid hormone, KTP = kidney transplantation
MEN = multiple endocrine neoplasia.

calculation, the radioactivity of Tc-99m sestamibi in the syringe was measured by a dose calibrator (CRC-15R, CAPINTEC) before and after the injection. The dose calibrator and the SPECT/CT scanners were cross-calibrated before the study. The cross-calibration factors of the 2 SPECT/CT scanners were comparable to each other: 152.5 cpm/μCi (Oct 2015–Aug 2017) and 151.8 cpm/μCi (Sep 2017–Oct 2017) for the NMCT670 and 152.8 cpm/μCi for the NMCT670Pro. The times of radioactivity measurement and injection were recorded and used for the SUV calculation. SPECT images were acquired from the mandible to mediastinum using the following parameters: step-and-shoot mode (10 s/step, 3 degree angle, and total 120 steps (60 steps per detector)) with the body contour option, the energy window peak at 140 KeV (20% window of 126–154 KeV), the scatter window peak at 120 KeV (10% window of 115–125 KeV), and a zoom factor of 1.5. Spiral CT was performed using a tube voltage of 120 KVp, tube current of 30 mA, X-ray collimation of 20 mm (16 × 1.25 mm), table speed of 37 mm/s, table feed per rotation of 18.75 mm/rot, tube rotation time of 0.5 s, and pitch of 0.938:1. CT images were reconstructed using an adaptive statistical iterative reconstruction algorithm (ASiR, GE Healthcare) into trans-axial slices of 2.5 mm thickness and an image matrix of 512 × 512. SPECT images were reconstructed using an ordered-subset expectation maximization algorithm with 2 iterations and 10 subsets into a 128 × 128 matrix and slice thickness of 2.95 mm. During the SPECT image reconstruction, 3 corrections for radioactivity (CT-attenuation correction, scatter correction, and resolution recovery) were used.

2.3. Parameters of the quantitative SPECT/CT

Circular regions-of-interest (ROIs) were manually drawn slice-by-slice over the parathyroid lesions on the trans-axial CT images, and the ROIs were automatically reflected on the SPECT/CT images by the Q.Metrix software. Volumes of interest (VOIs) were generated by integrating the ROIs. For a given VOI, the maximum standardized uptake value (SUVmax), and mean SUV (SUVmean) were calculated using the following equations in the Q.Metrix software.

$$\mathrm{SUVmax} = \frac{Highest\ radioactivity\ in\ a\ voxel / Voxel\ volume}{Injected\ radioactivity / Body\ weight}(g/mL)$$

$$\mathrm{SUVmean} = \frac{Mean\ radioactivity\ in\ a\ VOI / VOI\ volume}{Injected\ radioactivity / Body\ weight}(g/mL)$$

The VOI volume was 2.53 ± 7.23 mL (range: 0.2–46.2 mL); the voxel volume of the current SPECT/CT protocol was set as 3.2×10^{-3} mL.

The thyroid was employed as a reference tissue; a circular ROI was placed at the middle lobe of contralateral thyroid. The method of SUV measurement is presented in Figure 1.

2.4. Pathology of parathyroid tissues

The resected parathyroid gland specimens were fixed with 10% buffered formalin. After macroscopic examination, the specimens were cut serially into 3 to 4 mm slices. These sections were embedded in paraffin at room temperature for 24 hour, and cut

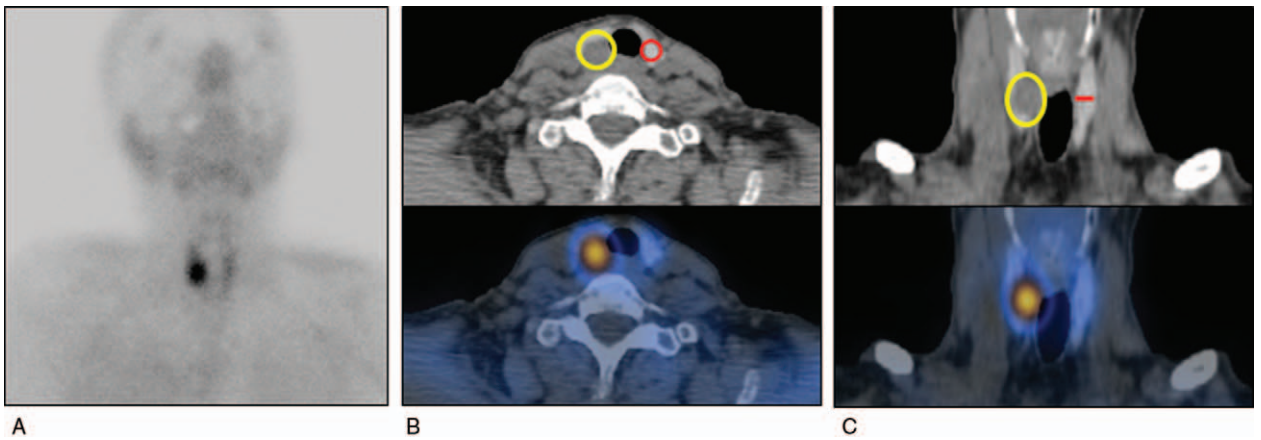

Figure 1. Measuring the standardized uptake value. (A) Planar anterior image showing a Tc-99m sestamibi uptake-positive lesion in the right thyroid area. (B) Trans-axial images displaying circular regions-of-interest (ROIs) in a parathyroid lesion (yellow) and the reference contralateral thyroid (red). (C) Coronal images revealing a volume-of-interest for the parathyroid lesion (yellow) and a single ROI for the reference (red).

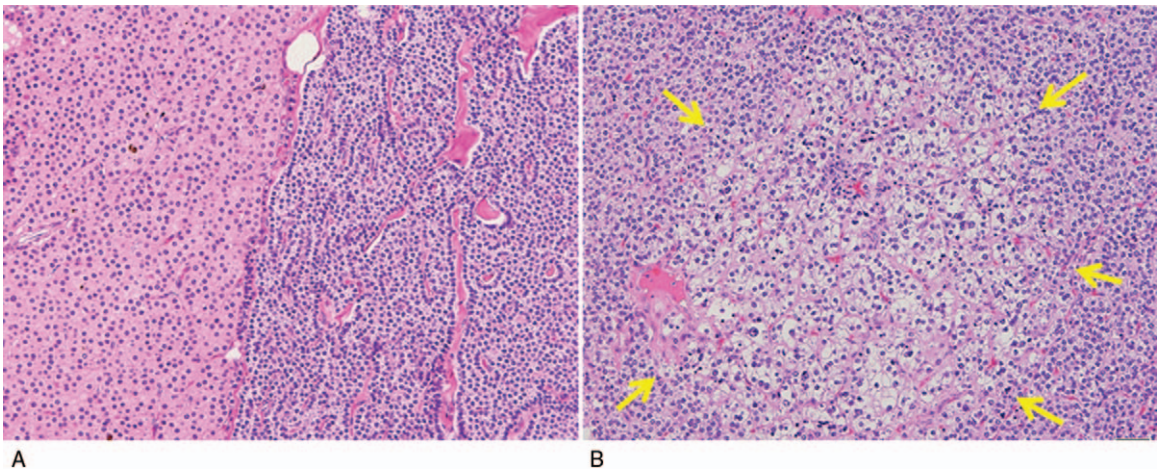

Figure 2. Representative figure showing three types of cells. (A) The right half shows chief cells with pale to eosinophilic scant cytoplasm. The left half shows oxyphilic cells with abundant bright eosinophilic cytoplasm. (B) The center shows cells with optically clear cytoplasm (clear cells) (arrows). The nuclei of clear cells are small and located either centrally or acentric. The chief cells are surrounding the clear cells (x200 magnification).

into 4-μm sections. Subsequently, hematoxylin eosin staining was performed. First, the sections were deparaffinized with > 99% xylene, followed by hydration using decreasing concentrations of alcohol and water (100, 90, 80 and 70%). Then the sections were stained in hematoxylin solution for 5 minute at room temperature and washed with water for 3 minute. After adding 1% acid alcohol for 5 minute and washing in running tap water, the sections were stained with 1% eosin for 10 minute and were washed again in tap water for 5 minute. Finally, the sections were dehydrated using increasing concentrations (85, 90, 95, 10 and 100%) of alcohols and > 99% xylene.

The slides of parathyroid adenomas and hyperplasia were reviewed by 2 experienced pathologists (HYN and SYP) in a blind manner using light microscope (BX51, Olympus Corporation, Tokyo, Japan) (magnification x40, and x200). Diagnoses were confirmed by both clinical and operative results and histologic features of each lesion. The cellular proportion of the lesions was manually calculated by reviewing all slides without computer- or machine-based analytical program. The percentage of area of parathyroid cells (chief cells, oxyphil cells, and clear cells) was separately evaluated (Fig. 2). Disputed cases were discussed for consensus.

2.5. Statistical analysis

Statistical analyses were performed using MedCalc statistical software (version 17.4, MedCalc Software, Mariakerke, Belgium), except for the 2-way repeated-measures analysis of variance (ANOVA) test (GraphPad Prism version 6.01, GraphPad Software Inc.). The 2-way repeated-measures ANOVA and Tukey's multiple comparison tests were performed to evaluate the SUV difference along the early and delayed phases. Group comparisons between the adenomas, hyperplasia, and reference thyroid tissue were analyzed using the Kruskall-Wallis test with post-hoc analysis because the assumption of equal variances was refused by Levene's test. Receiver operating characteristics (ROC) analysis was employed to find the optimal SUV cutoff: we tested the 4 SUV parameters (SUVmax_D = SUVmax at the delayed phase, SUVmean_D = SUVmean at the delayed phase, SUVmax_E = SUVmax at the early phase, and SUVmean_E = SUVmean at the early phase) in variable circumstances. The relations between quantitative SPECT/CT parameters and pathologic results were evaluated using the rank correlation analysis of Spearman's rho. The group comparison of pathologic data between the adenomas and hyperplasia was conducted using the Mann-Whitney test because the assumption of equal variance was rejected by an *F*-test. A *P*-value of $< .05$ was considered statistically significant.

3. Results

3.1. Quantitative parameters of SPECT/CT

For all parathyroid lesions and reference thyroid tissues, the SUVs decreased from the early SPECT/CT to the delayed SPECT/CT (Fig. 3). At the early SPECT/CT, the SUVs were different among the 3 lesions, and post-hoc analyses confirmed that the adenomas showed significantly greater SUV than the hyperplasia and reference ($P < .05$ each) (Table 2). At the delayed SPECT/CT, the SUVs were also different among the 3 lesions. Post-hoc analyses showed that the SUVmax at the delayed phase was significantly different among the 3 lesions, decreasing gradually from the adenomas to the hyperplasia to the reference ($p < .05$ for all pairwise comparisons). The SUVmean at the delayed phase was significantly lower in the reference than in the adenomas and hyperplasia ($P < .05$), but the adenomas and the hyperplasia did not differ each other ($P > .05$) (Table 2). All the above statistical analyses were reflected in repeated-measures ANOVA tests: the adenomas had significantly higher SUVs than the hyperplasia and reference thyroid tissue along the early and delayed phases (Fig. 3). Notably, the hyperplasia was not significantly different from the reference tissue along the early and delayed phases using repeated-measures ANOVA tests (Fig. 3).

3.2. Optimal quantitative parameter of SPECT/CT for identification of adenoma or hyperplasia

An SUVmax_D cutoff of 3.26 was the most significant identifier for the identification/differentiation of parathyroid adenoma among the SUV parameters ($P = .0217$ for SUVmax_D versus SUVmean_D; $P < .001$ for SUVmax_D versus other SUVs,

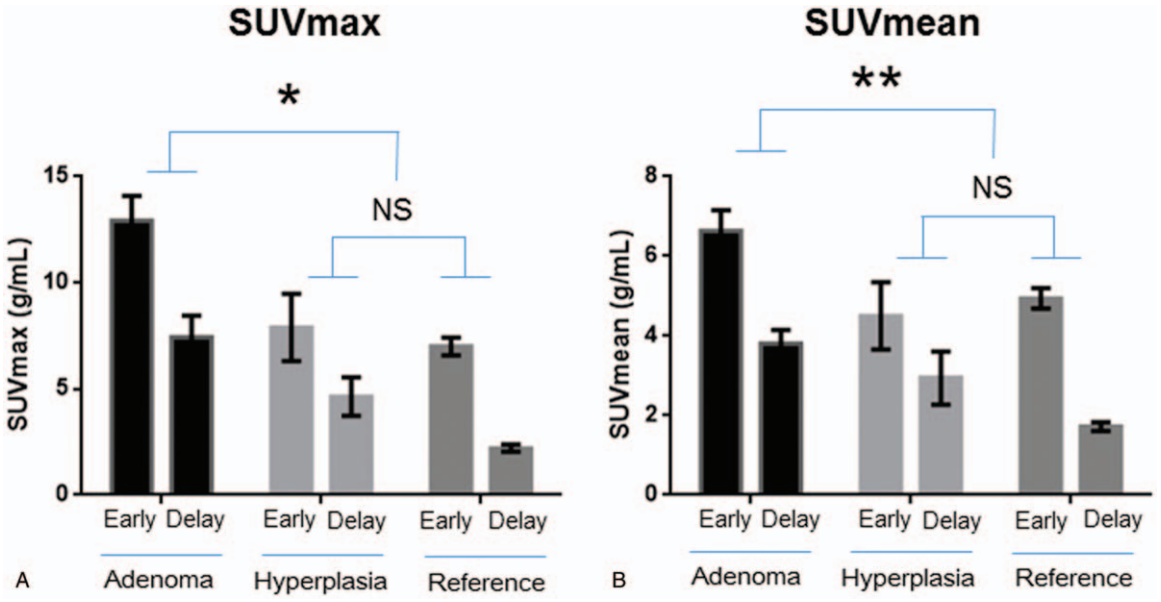

Figure 3. Quantitative SPECT/CT parameters along the early and delayed phases. (A) The SUVmax of the parathyroid adenomas were significantly greater than those of the hyperplasia and reference thyroid (*; $P=.0131$ between the adenomas and hyperplasia and $P<.0001$ between the adenomas and reference). However, the parathyroid hyperplasia did not show significant SUVmax difference from the reference thyroid (NS; $P=.4196$). (B) The SUVmean showed a similar pattern. Adenomas had significantly greater SUVmean than the hyperplasia and reference (**; $P=.0486$ between the adenomas and hyperplasia and $P=.0001$ between the adenomas and reference), while the hyperplasia and reference did not show SUVmean difference between them (NS; $P=.7949$). Data are presented as mean ± standard error of mean. NS: non-significant; SUVmax: maximum standardized uptake value; SUVmean: mean standardized uptake value.

Table 3 and Fig. 4). In case of differential diagnosis, excluding the reference, between parathyroid adenoma versus hyperplasia, an SUVmax_D cutoff of 7.13 worked with a sensitivity of 50.0% and a specificity of 92.86% (Table 3).

Figure 5 demonstrates representative Tc-99m sestamibi scintigraphy (planar and SPECT/CT) images that show the SUVmax difference in the early and delayed phases between the parathyroid adenomas, hyperplasia, and reference thyroid tissues.

3.3. Correlations between SUVs and pathologic cell proportions

The volume of the parathyroid adenomas was larger than that of the hyperplasia, although not statistically significant ($P=.1436$). The adenomas had significantly higher chief cell proportions and lower oxyphil cell proportions than the hyperplasia ($P=.0064$ and $P=.0054$, respectively). The clear cell proportions were not different between the adenomas and hyperplasia ($P=.6341$) (Table 4). In the adenomas, the SUVmax_D had a negative correlation with the PTH-producing chief cell proportion ($P=.0294$) and a positive correlation with the mitochondria-abundant oxyphil cell proportion ($P=.0173$). However, in the hyperplasia, no correlation was observed between SUVmax_D and any cellular proportions (chief cells: $P=.7500$, oxyphil cells: $P=.4373$) (Fig. 6).

In the adenoma, the SUVmean_D had a negative correlation with the chief cells ($P=.0010$) and a positive correlation with the oxyphil cells ($P=.0080$) like SUVmax_D, whereas the SUVmax_E and SUVmean_E failed to show significant correlation with either chief cells ($P=.3410$, $P=.1434$, respectively) or oxyphil cells ($P=.3158$, $P=.1455$, respectively). In the hyperplasia, SUVmax_E, SUVmean_E, and SUVmean_D had no significant correlation with any cellular proportions (chief cells: $P=.3381$, $P=.4317$, $P=.6211$, respectively; oxyphil cells: $P=.4451$, $P=.4787$, $P=.8441$, respectively).

For the clear cells, no correlation was observed between SUVs and the cellular proportions.

Table 2

SUVmax and SUVmean of parathyroid lesions and the reference thyroid tissue.

		SUVmax (g/mL)		SUVmean (g/mL)	
		Early	Delayed	Early	Delayed
Adenoma (n=32)		12.92±6.68	7.46±5.66	6.63±2.99	3.81±1.94
Hyperplasia (n=12)		7.90±5.49	4.65±3.14	4.50±2.91	2.95±2.32
Reference (n=39)		7.01±2.62	2.21±1.07	4.94±1.62	1.73±0.68
Kruskal-Wallis test	*P*-value	<.0001	<.0001	.0122	<.0001
	Post-hoc analysis ($P<.05$)	Adenoma vs others	Adenoma vs hyperplasia vs reference	Adenoma vs others	Others vs reference

SUVmax: maximum standardized uptake value.
SUVmean: mean standardized uptake value.
Data are presented as mean ± standard deviation.

Table 3

The area under the curve (AUC) of receiver operating characteristics (ROC) analyses for SUV parameters regarding the identification of parathyroid lesions.

	Hyperparathyroid lesions* vs reference (n = 83)	Adenoma vs reference (n = 71)	Hyperplasia vs reference (n = 51)	Adenoma vs hyperplasia (n = 44)
SUVmax_D	0.892 (0.804 to 0.949, $P < .0001$)	0.919 (0.830 to 0.971, $P < .0001$)	0.817 (0.684 to 0.912, $P < .0001$)	0.702 (0.545 to 0.830, $P = .0199$)
SUVmean_D	0.818 (0.718 to 0.894, $P < .0001$)	0.856 (0.753 to 0.928, $P < .0001$)	0.716 (0.572 to 0.833, $P = .0287$)	0.676 (0.518 to 0.809, $P = .0576$)
SUVmax_E	0.726 (0.617 to 0.818, $P = .0001$)	0.817 (0.707 to 0.898, $P < .0001$)	0.516 (0.372 to 0.658, $P = .8846$)	0.763 (0.611 to 0.878, $P = .0019$)
SUVmean_E	0.575 (0.461 to 0.683, $P = .2389$)	0.660 (0.538 to 0.768, $P = .0164$)	0.653 (0.507 to 0.781, $P = .1474$)	0.729 (0.574 to 0.852, $P = .0133$)

* Hyperparathyroid lesions: adenomas plus hyperplasia
SUVmax_D: maximum SUV at the delayed phase
SUVmean_D: mean SUV at the delayed phase
SUVmax_E: maximum SUV at the early phase
SUVmean_E: mean SUV at the early phase
Values in parentheses indicate 95% confidence intervals of the AUCs and p values.

4. Discussion

The main result of this study is that the uptake of Tc-99m sestamibi in parathyroid lesions can be quantified by SPECT/CT technology, and the quantitative parameter (SUVmax_D) was accurate enough to identify the parathyroid lesions causing hyperparathyroidism. Notably, the delayed imaging, not the early imaging, proved to be the most relevant for identifying the underlying cause of hyperparathyroidism. Thus, traditional dual-phase imaging might not be required if the SUVmax could be calculated at the delayed phase SPECT/CT.[14,18] In fact, early phase imaging has usually been used as an anatomical reference to locate parathyroid lesions that showed persistent Tc-99m sestamibi uptake in the delayed planar images that often lack a thyroid landmark.[11,18,32] The absolute value of SUVmax was greater at the early phase than at the delayed phase, but the identification of parathyroid lesions was more effective at the delayed phase.

The parathyroid adenomas and hyperplasia could be differentiated from each other using the SUVmax_D, and the SUVmax_D difference could be explained by the different cellular compositions. Generally, parathyroid hyperplasia has been considered indistinguishable from parathyroid adenomas by microscopy alone. Only multiplicity is widely accepted as a clinical criterion for parathyroid hyperplasia.[33–35] Mitochondrial DNA mutation was reported to be different between adenomas and hyperplasia, but the clinical significance remains unclear.[36] Here, the degree of Tc-99m sestamibi uptake was clearly different between the adenomas and hyperplasia, and the adenomas showed correlations between its SUVmax_D and the cellular proportions, but the hyperplasia did not. In adenomas, the proportion of oxyphil cells was positively correlated with the SUVmax_D, which reflects the known uptake mechanism of Tc-99m sestamibi in the mitochondria-abundant cells.[11,37,38] The oxyphil cells play a minor role in the phenotype of hyperparathyroidism because they do not secrete PTH, but due to the high mitochondrial content, positive uptake occurs during Tc-99m sestamibi scintigraphy.[39,40] The reason for the negative correlation between the SUVmax_D and the chief cell proportions can be explained as the reciprocal phenomenon of the positive correction between the SUVmax_D and the oxyphil cell proportions because not absolute but relative cellular proportions were assessed by the pathologists: the higher oxyphil cell proportions resulted in the lower chief cell proportions, and vice versa.

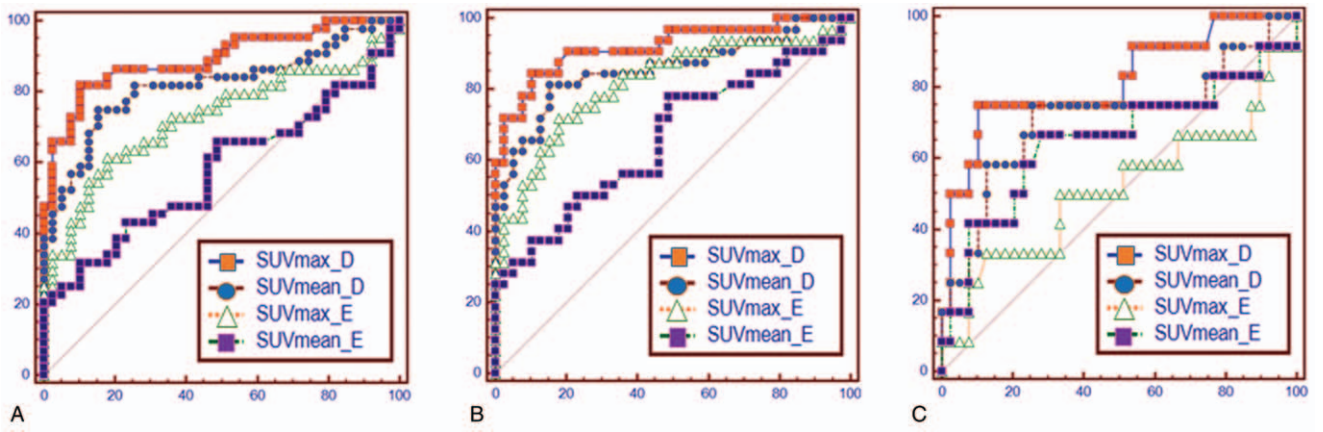

Figure 4. ROC curve analyses of SUV parameters for the identification of parathyroid lesions. (A) For hyperparathyroidism (adenomas plus hyperplasia) versus reference, the SUVmax_D cutoff of 3.26 yielded a sensitivity of 81.82% and a specificity of 89.74% ($P = .0014$ for SUVmax_D versus SUVmean_D; $P < .0001$ for SUVmax_D versus other SUVs, n = 83). (B) For adenomas versus reference, the SUVmax_D of 3.26 resulted in a sensitivity of 84.37% and a specificity of 89.74% ($P = .0217$ for SUVmax_D versus SUVmean_D; $P < .001$ for SUVmax_D versus other SUVs, n = 71). (C) For hyperplasia versus reference, the SUVmax_D of 3.26 had a sensitivity of 75.00% and a specificity of 89.74% ($P = .1796$ for SUVmax_D versus SUVmean_D; $P > .01$ for SUVmax_D versus other SUVs, n = 51). SUVmax_D: maximum standardized uptake value (SUV) at the delayed phase; SUVmax_E: maximum SUV at the early phase; SUVmean_D: mean SUV at the delayed phase; SUVmean_E: mean SUV at the early phase.

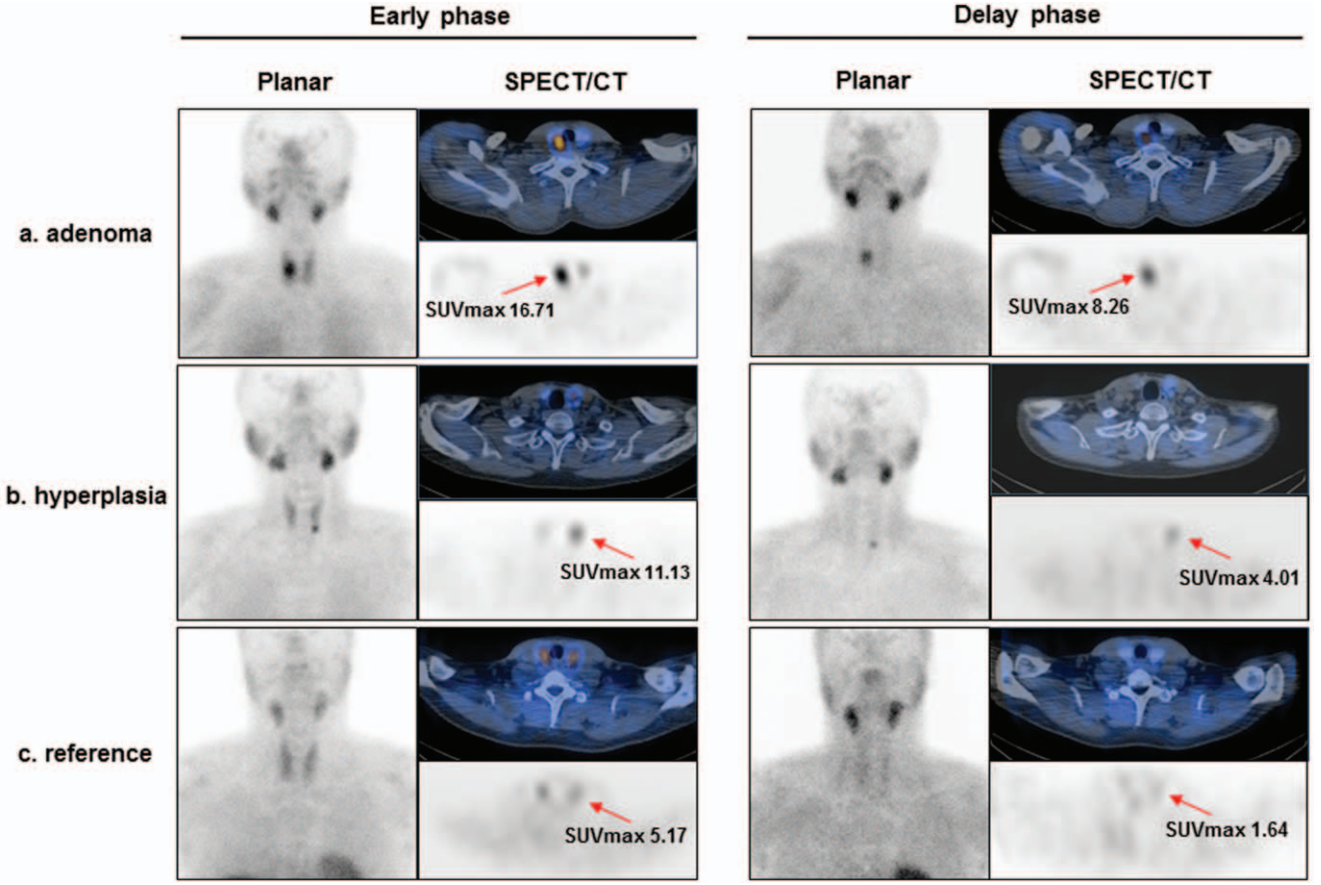

Figure 5. Representative Tc-99m sestamibi scintigraphy (anterior planar and transaxial SPECT/CT) images in the early and delayed phases. (A) Single adenoma (size, $2.2 \times 1.0 \times 0.7$ cm) was confirmed in the right thyroid lobe area by surgery in a 66-yr-old male patient. (B) A hyperplasia lesion (size, $1.1 \times 1.0 \times 0.6$ cm) was confirmed in the left lower thyroid lobe area by surgery in a 48-yr-old male patient with type 1 multiple endocrine neoplasia. (C) Reference tissue was selected in the left thyroid lobe in a 42-yr-old male patient with no thyroid or parathyroid lesion in the left thyroid area. SUVmax: maximum standardized uptake value.

The current study results were highly compatible with previous reports that had revealed higher SUVmax of the adenoma compared with that of the reference (2.71 ± 0.58 versus 1.74 ± 0.62, $P = .007$[41] or 3.40 ± 3.09 versus 1.84 ± 1.05, $P < .001$[42]) in the delayed SPECT/CT, although the absolute levels of SUVmax were lower than our study results. Regarding the early phase SUVmax, the previous studies showed contradictory findings,[41,42] which might be reflected by our study results that the SUVmax_E was less potent than the SUVmax_D for adenoma identification.

The limitations of the study design necessitate careful interpretation of the results. First, 1 critical drawback is that only Tc-99m sestamibi positive lesions were included in the study. For example, all the hyperplasia patients had 3 or 4 hyperplasia lesions, but only 1 lesion per patient was visualized in 71.4% (5/7) of the patients. Therefore, the results may have overestimated the actual sensitivity. Second, pathologic evaluations were not absolutely quantitative because cellular proportions were examined without consideration of the real tumor size. This might explain the absence of a positive correlation in the hyperplasia between the proportion of oxyphil cells and the SUVmax. Last, the number of hyperplasia lesions was relatively small compared to that of adenomas. The imbalance may have caused a false generalization to hyperplasia. Therefore, a larger number of lesions and a prospective study design are required in future studies.

Table 4

Pathologic characteristics of the parathyroid lesions (n = 44).

		Adenoma (n = 32)	Hyperplasia (n = 12)	*P*-value
Volume (cm^3)		2.64 ± 7.57	1.66 ± 0.95	.1436
Cellular proportion (%)	Chief cell	82.28 ± 29.45	75.42 ± 15.59	.0064
	Oxyphil cell	16.91 ± 29.69	20.42 ± 11.37	.0054
	Clear cell	0.81 ± 2.24	4.17 ± 14.43	.6341

Data are presented as mean ± standard deviation.

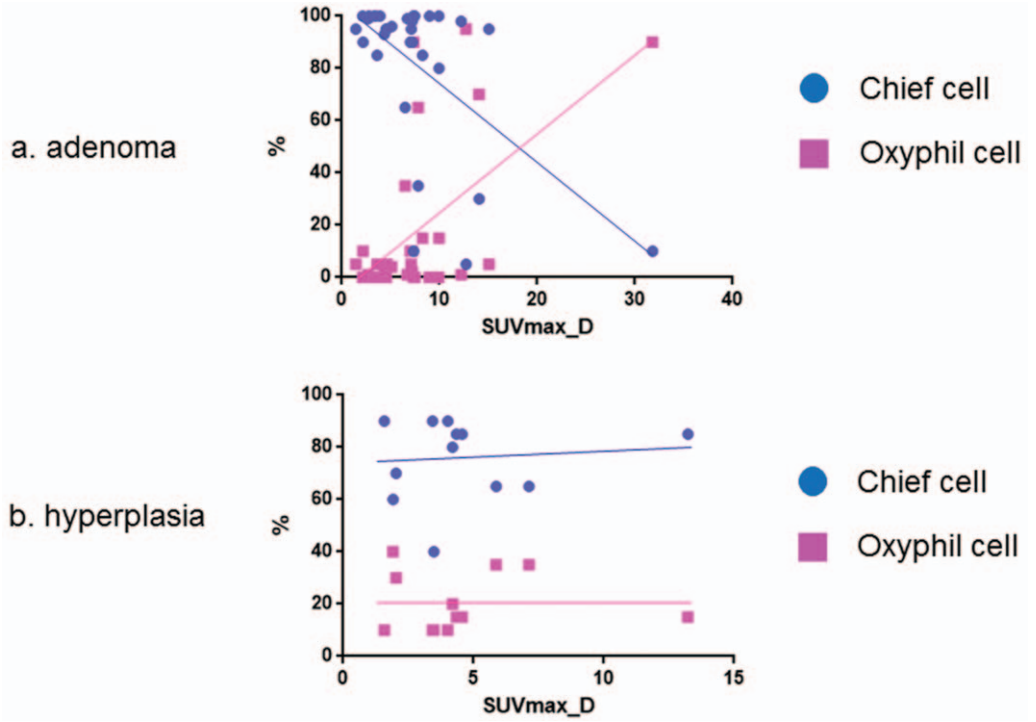

Figure 6. Correlations between the SUVmax at the delayed phase (SUVmax_D) and pathologic cellular proportions. (A) In the parathyroid adenomas, the SUVmax_D had a negative correlation with the PTH-producing chief cell proportion (rho = -0.385, 95% confidence interval (CI):-0.647-0.0424, $P = .0294$) and a positive correlation with the mitochondria-abundant oxyphil cell proportion (rho = 0.418, 95% CI: 0.0811– 0.669, $P = .0173$). (B) In the parathyroid hyperplasia, the SUVmax_D was not correlated with the chief cell (rho = -0.103, 95% CI: -0.639–0.500, $P = .7500$) and oxyphil cell (rho = 0.248, 95% CI: -0.380–0.719, $P = .4373$) proportions.

5. Conclusion

Quantitative Tc-99m sestamibi SPECT/CT may provide surgeons with objective criteria for the identification/differentiation of parathyroid lesions causing hyperparathyroidism. Taken with the findings above, the SUVmax at the delayed SPECT/CT may be accurate enough to identify the culprit parathyroid lesions.

Acknowledgments

We would like to thank Editage (www.editage.co.kr) for English language editing.

Author contributions

Conceptualization: So Yeon Park, June Young Choi, Young So, Won Woo Lee.
Data curation: Hee Young Na, June Young Choi, Won Woo Lee.
Formal analysis: Hoon Young Suh, Hee Young Na, June Young Choi, Young So, Won Woo Lee.
Funding acquisition: Won Woo Lee.
Investigation: Hee Young Na, So Yeon Park, Won Woo Lee.
Methodology: Hoon Young Suh, Hee Young Na, So Yeon Park, Young So, Won Woo Lee.
Project administration: Hoon Young Suh, So Yeon Park, Young So, Won Woo Lee.
Resources: Hoon Young Suh, Hee Young Na, June Young Choi, Won Woo Lee.
Software: Hoon Young Suh, Hee Young Na, June Young Choi, Won Woo Lee.
Supervision: So Yeon Park, June Young Choi, Young So, Won Woo Lee.
Validation: So Yeon Park, June Young Choi, Young So, Won Woo Lee.
Visualization: So Yeon Park, June Young Choi, Young So, Won Woo Lee.
Writing – original draft: Won Woo Lee.
Writing – review & editing: Won Woo Lee.

References

[1] Ruda JM, Hollenbeak CS, Stack BCJr. A systematic review of the diagnosis and treatment of primary hyperparathyroidism from 1995 to 2003. Otolaryngol Head Neck Surg 2005;132:359–72.
[2] Thakker RV, Newey PJ, Walls GV, et al. Clinical practice guidelines for multiple endocrine neoplasia type 1 (MEN1). J Clin Endocrinol Metab 2012;97:2990–3011.
[3] Wasserman JD, Tomlinson GE, Druker H, et al. Multiple endocrine neoplasia and hyperparathyroid-jaw tumor syndromes: clinical features, genetics, and surveillance recommendations in childhood. Clin Cancer Res 2017;23:e123–32.
[4] Insogna KL. Primary Hyperparathyroidism. N Engl J Med 2018;379: 1050–9.
[5] de Francisco AL. Secondary hyperparathyroidism: review of the disease and its treatment. Clin Ther 2004;26:1976–93.
[6] Locatelli F. The need for better control of secondary hyperparathyroidism. Nephrol Dial Transplant 2004;19(Suppl 5):V15–9.
[7] Bilezikian JP, Brandi ML, Eastell R, et al. Guidelines for the management of asymptomatic primary hyperparathyroidism: summary statement from the Fourth International Workshop. J Clin Endocrinol Metab 2014;99:3561–9.
[8] Marcocci C, Bollerslev J, Khan AA, et al. Medical management of primary hyperparathyroidism: proceedings of the fourth International Workshop on the Management of Asymptomatic Primary Hyperparathyroidism. J Clin Endocrinol Metab 2014;99:3607–18.

[9] Greenspan BS, Dillehay G, Intenzo C, et al. SNM practice guideline for parathyroid scintigraphy 4.0. J Nucl Med Technol 2012;40:111–8.
[10] Coakley AJ, Kettle AG, Wells CP, et al. 99Tcm sestamibi–a new agent for parathyroid imaging. Nucl Med Commun 1989;10:791–4.
[11] O'Doherty MJ, Kettle AG, Wells P, et al. Parathyroid imaging with technetium-99m-sestamibi: preoperative localization and tissue uptake studies. J Nucl Med 1992;33:313–8.
[12] Krausz Y, Bettman L, Guralnik L, et al. Technetium-99m-MIBI SPECT/CT in primary hyperparathyroidism. World J Surg 2006;30:76–83.
[13] Thomas DL, Bartel T, Menda Y, et al. Single photon emission computed tomography (SPECT) should be routinely performed for the detection of parathyroid abnormalities utilizing technetium-99m sestamibi parathyroid scintigraphy. Clin Nucl Med 2009;34:651–5.
[14] Ciappuccini R, Morera J, Pascal P, et al. Dual-phase 99mTc sestamibi scintigraphy with neck and thorax SPECT/CT in primary hyperparathyroidism: a single-institution experience. Clin Nucl Med 2012;37: 223–8.
[15] Lavely WC, Goetze S, Friedman KP, et al. Comparison of SPECT/CT, SPECT, and planar imaging with single- and dual-phase (99m)Tc-sestamibi parathyroid scintigraphy. J Nucl Med 2007;48:1084–9.
[16] Nichols KJ, Tomas MB, Tronco GG, et al. Preoperative parathyroid scintigraphic lesion localization: accuracy of various types of readings. Radiology 2008;248:221–32.
[17] Wei WJ, Shen CT, Song HJ, et al. Comparison of SPET/CT, SPET and planar imaging using 99mTc-MIBI as independent techniques to support minimally invasive parathyroidectomy in primary hyperparathyroidism: a meta-analysis. Hell J Nucl Med 2015;18:127–35.
[18] Taillefer R, Boucher Y, Potvin C, et al. Detection and localization of parathyroid adenomas in patients with hyperparathyroidism using a single radionuclide imaging procedure with technetium-99m-sestamibi (double-phase study). J Nucl Med 1992;33:1801–7.
[19] Bailey DL, Willowson KP. An evidence-based review of quantitative SPECT imaging and potential clinical applications. J Nucl Med 2013;54: 83–9.
[20] Cachovan M, Vija AH, Hornegger J, et al. Quantification of 99mTc-DPD concentration in the lumbar spine with SPECT/CT. EJNMMI Res 2013;3:45.
[21] Suh MS, Lee WW, Kim YK, et al. Maximum standardized uptake value of (99m)Tc Hydroxymethylene Diphosphonate SPECT/CT for the evaluation of temporomandibular joint disorder. Radiology 2016;280: 890–6.
[22] Lee H, Kim JH, Kang YK, et al. Quantitative single-photon emission computed tomography/computed tomography for technetium pertechnetate thyroid uptake measurement. Medicine (Baltimore) 2016;95: e4170.
[23] Kim J, Lee HH, Kang Y, et al. Maximum standardised uptake value of quantitative bone SPECT/CT in patients with medial compartment osteoarthritis of the knee. Clin Radiol 2017;72:580–9.
[24] Kim HJ, Bang JI, Kim JY, et al. Novel application of quantitative single-photon emission computed tomography/computed tomography to predict early response to methimazole in graves' disease. Korean J Radiol 2017;18:543–50.
[25] Kang YK, Park S, Suh MS, et al. Quantitative single-photon emission computed tomography/computed tomography for glomerular filtration rate measurement. Nucl Med Mol Imaging 2017;51:338–46.
[26] Kim JY, Kim JH, Moon JH, et al. Utility of quantitative parameters from single-photon emission computed tomography/computed tomography in patients with destructive thyroiditis. Korean J Radiol 2018;19:470–80.
[27] Kim J, Lee H, Lee H, et al. Quantitative single-photon emission computed tomography/computed tomography for evaluation of salivary gland dysfunction in sjogren's syndrome patients. Nucl Med Mol Imaging 2018;52:368–76.
[28] Lee R, So Y, Song YS, et al. Evaluation of hot nodules of thyroid gland using Tc-99m Pertechnetate: a novel approach using quantitative single-photon emission computed tomography/computed tomography. Nucl Med Mol Imaging 2018;52:468–72.
[29] Bae S, Kang Y, Song YS, et al. Maximum standardized uptake value of foot SPECT/CT using Tc-99m HDP in patients with accessory navicular bone as a predictor of surgical treatment. Medicine (Baltimore) 2019;98: e14022.
[30] Ryoo HG, Lee WW, Kim JY, et al. Minimum standardized uptake value from quantitative bone single-photon emission computed tomography/computed tomography for evaluation of femoral head viability in patients with femoral neck fracture. Nucl Med Mol Imaging 2019;53: 287–95.
[31] Lee WW, Group KS. Clinical applications of technetium-99m quantitative single-photon emission computed tomography/computed tomography. Nucl Med Mol Imaging 2019;53:172–81.
[32] Nguyen BD. Parathyroid imaging with Tc-99m sestamibi planar and SPECT scintigraphy. Radiographics 1999;19:601–14.
[33] Johnson SJ, Sheffield EA, McNicol AM. Best practice no 183, Examination of parathyroid gland specimens. J Clin Pathol 2005;58:338–42.
[34] Johnson NA, Tublin ME, Ogilvie JB. Parathyroid imaging: technique and role in the preoperative evaluation of primary hyperparathyroidism. AJR Am J Roentgenol 2007;188:1706–15.
[35] Bahl M, Sepahdari AR, Sosa JA, et al. Parathyroid adenomas and hyperplasia on four-dimensional CT scans: three patterns of enhancement relative to the thyroid gland justify a three-phase protocol. Radiology 2015;277:454–62.
[36] Costa-Guda J, Tokura T, Roth SI, et al. Mitochondrial DNA mutations in oxyphilic and chief cell parathyroid adenomas. BMC Endocr Disord 2007;7:8.
[37] Chiu ML, Kronauge JF, Piwnica-Worms D. Effect of mitochondrial and plasma membrane potentials on accumulation of hexakis (2-methoxyisobutylisonitrile) technetium(I) in cultured mouse fibroblasts. J Nucl Med 1990;31:1646–53.
[38] Arbab AS, Koizumi K, Toyama K, et al. Uptake of technetium-99m-tetrofosmin, technetium-99m-MIBI and thallium-201 in tumor cell lines. J Nucl Med 1996;37:1551–6.
[39] Giorgadze T, Stratton B, Baloch ZW, et al. Oncocytic parathyroid adenoma: problem in cytological diagnosis. Diagn Cytopathol 2004;31: 276–80.
[40] Paul A, Villepelet A, Lefevre M, et al. Oncocytic parathyroid adenoma. Eur Ann Otorhinolaryngol Head Neck Dis 2015;132:301–3.
[41] Razavi S, Ziebarth B, Klein R, et al. Dual time-point quantitative SPECT-CT parathyroid imaging using a single computed tomography: feasibility and operator variability. Nucl Med Commun 2018;39:3–9.
[42] Robin P, Klein R, Gardner J, et al. Quantitative analysis of technetium-99m-sestamibi uptake and washout in parathyroid scintigraphy supports dual mechanisms of lesion conspicuity. Nucl Med Commun 2019;40: 469–76.